Study on the optimization of the water Cherenkov detector array of the LHAASO project for surveying VHE gamma ray sources*

LI Hui-Cai(李会财)[1;2] CHEN Ming-Jun(陈明君)[2] JIA Huan-Yu(贾焕玉)[1] GAO Bo(高博)[2]
WU Han-Rong(吴含荣)[2] YAO Zhi-Guo(姚志国)[2] YUO Xiao-Hao(游晓浩)[2;3]
ZHOU Bin(周斌)[2] ZHU Feng-Rong(祝凤荣)[1]

[1] School of Physical Science and Technology, Southwest Jiaotong University, Chengdu 610031, China
[2] Institute of High Energy Physics, Chinese Academy of Sciences, Beijing 100049, China
[3] Normal University of Hebei, Shijiazhuang 050016, China

Abstract: It is prpopsed that a water Cherenkov detector array, LHAASO-WCDA, is to be built at Shangri-la, Yunnan Province, China. As one of the major components of the LHAASO project, the main purpose of it is to survey the northern sky for gamma ray sources in the energy range of 100 GeV–30 TeV. In order to design the water Cherenkov array efficiently to economize the budget, a Monte Carlo simulation is carried out. With the help of the simulation, the cost performance of different configurations of the array are obtained and compared with each other, serving as a guide for the more detailed design of the experiment in the next step.

Key words: LHAASO-WCDA, gamma rays source, cost performance, optimization

PACS: 96.50.sd, 07.85.-m **DOI:** 10.1088/1674-1137/38/1/016002

1 Introduction

The detection of Very-High-Energy (VHE, > 100 GeV) cosmic gamma rays has been campaigned vigorously for since the first detection of TeV gamma radiations from the Crab Nebula by the Whipple experiment in 1989 [1]. Two major detection approaches exist in this research field: Imaging Air Cherenkov Telescopes (IACTs) [2] and ground particle detector arrays [3]. The former wins in angular resolution ($<0.1^\circ$) and background rejection power, it possesses a better sensitivity in morphology observation and spectrum measurement. However, because of the low duty-circle (∼10%) and its narrow field of view ($<5^\circ$ typically), the IACT's capability in a full sky survey and the long-term monitoring of sources is very limited. This aspect is fortunately complemented by ground particle arrays, which can work all the time (duty cycle > 95%) and monitor a large piece of the sky ($>2\pi/3$) simultaneously, as shown by precedent experiments such as Tibet ASγ, Milagro and ARGO-YBJ. One of the techniques used in this kind of approach, the water Cherenkov, has the unique advantage of a much better background rejection power than other options like the plastic scintillator and RPC, which is well demonstrated by simulations and has been verified by the Milagro experiment.

Targeting gamma astronomy in the energy band from 100 GeV to 30 TeV, the water Cherenkov detector array (WCDA) [4] of the Large High Altitude Air Shower Observatory (LHAASO) [5], covering an area 90000 m^2, has been proposed to be built at Shangri-la (4300 m a.s.l.), Yunnan, China. Building on the experience of the Milagro experiment, the current official configuration of the WCDA is 5 m×5 m cell-sized, incorporated in a single photomultiplier at a water depth of 4 m for each cell [4]. The simulation of the array in this configuration shows a very good performance in sensitivity to gamma ray sources, particularly at the energy band around 5 TeV. However, this is not necessarily the best configuration, for instance for gamma rays at low energies, especially when the cost factor is taken into account. This paper is just to carry out this study, to see what the best configuration of the array is in the sense of cost performance, via tuning the cell size, the water depth and the number of PMTs.

The optimization scheme is introduced in Section 2 and the optimization procedures and results based on Monte Carlo simulations are presented in Section 3.

2 Optimization scheme

To simplify the optimization procedure, some discontinuous values of the detector configuration parameters

Received 6 March 2013
* Supported by NSFC (11175147) and Knowledge Innovation Fund of IHEP, Beijing
1) E-mail: lihuicai@ihep.ac.cn

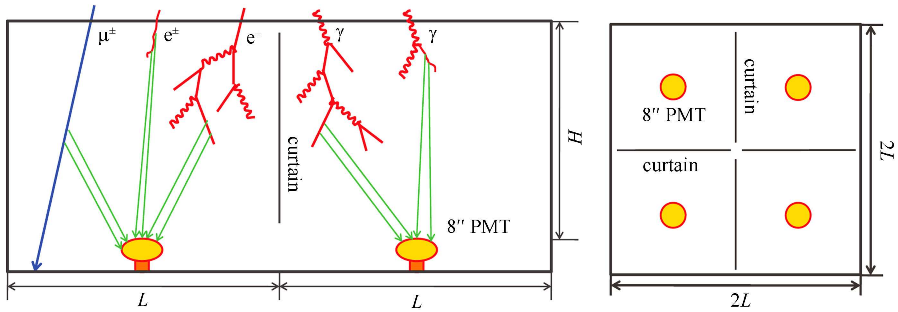

Fig. 1. Sketch drawing of four neighboring cell detectors. Left: side view; right: top view. Where L is the size of the cell and H is the water depth. As a diagramatic plot, only one PMT in each cell is drawn, which actually represents N PMTs.

regarding the cell size, the water depth and the number of PMTs in each cell are proposed to be taken as the starting point of the simulation. Fig. 1 shows the sketch drawing of four neighboring cell detectors in two view angles, where parameters L, H and N are subjected to be tuned. Three cell sizes, such as 4 m × 4 m, 5 m×5 m and 6 m×6 m, are selected; three effective water depths, such as 3 m, 4 m and 5 m, are chosen; five groups of PMT quantities in each cell, such as 1, 2, 3, 4 centered and 4 scattered, are adopted - as shown in Fig. 2, where the verbal adjectives of the last two groups with four PMTs represent where the four PMTs are located, near the center or much separated in the cell. Each iteration of these three kinds of elements can be combined to form a particular configuration. Altogether there are 3×3×5=45 configurations to be proceeded with, whose cost performances are duly evaluated and compared.

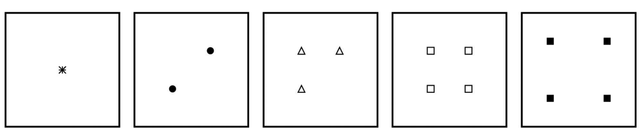

Fig. 2. Five groups of PMT quantities in a cell. ⁕: 1 PMT, •: 2 PMTs, △: 3 PMTs, □: 4 PMTs centered, ■: 4 PMTs scattered.

2.1 Simplified simulations

A full simulation should be the best approach for calculating the performance of each configuration, but in practice, it would be exhausted due to the fact that the simulation procedure is quite time-consuming, especially the process of production and tracing of the Cherenkov lights in the water. As to the array of the current design, which is just one example of the above 45 configurations, three months were taken with a PC farm of 100 CPU cores. In order to accomplish the optimization for all above configurations, years of computing time are expected. This is of course not a practical solution. To get over this obstacle, a simple and efficient optimization procedure is adopted and proceeded, as follows.

First of all, in order to lessen the burden of iterations in the simulation, for each cell, overall nine PMTs are put into the detector configuration at the same time, see Fig. 3. These nine PMTs can be easily classified afterwards in the off line into the five groups required for the optimization. This kind of overall configuration would not change the simulation results much, as the area of nine PMTs is very limited comparing the whole cell bottom, and as they react more-or-less like the surrounding curtains or plastics in black of each cell for the purpose of avoiding reflections of Cherenkov lights. With help of this treatment, the total number of iterations can be reduced to be 3×3=9.

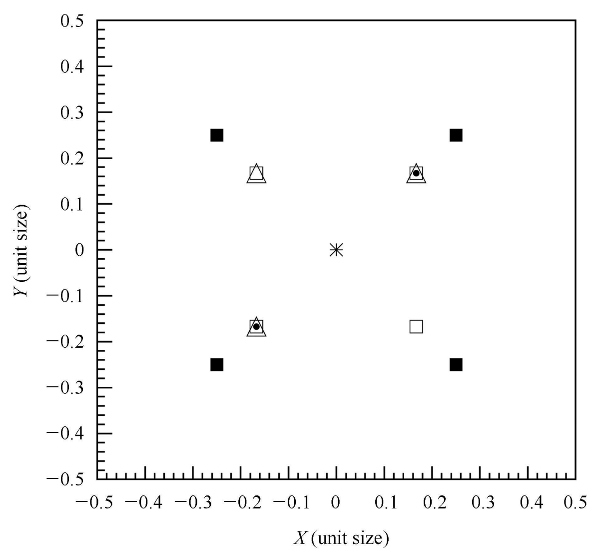

Fig. 3. PMT locations for simultaneous simulation of five groups of PMT quantities.

Special scenarios, which means simplified detector setups and/or simplified sets of primary shower parameters, like energy, direction and projection area, are adopted in the study for the sake of speeding up the simulation. What we are concerned with is the performance comparison between different detector configurations, which can be told by simulations in some special scenarios; the absolute performance values for real cases are important too but they are out of the scope of this study. After that, two simulation approaches dealing with two different special scenarios are carried out.

1) Single cell approach

As the simplest scenario, just a single cell detector is used for the simulation. Secondary particles of hundreds of primary gamma showers are thrown one by one onto the cell detector, then their interaction and transport processes in the water and in the PMT are simulated. Counting the number of particles that fired at least 1 PMT, compared with the number that were thrown onto the cell, the efficiency η of the cell detector is obtained. The efficiency for water Cherenkov is usually less than 30%, but ample photons in the shower secondary particles compensate for the loss of efficiency when comparing with other types of arrays, such as the plastic scintillator or RPCs that detect only charged particles. For the full coverage detector, if a major part of the shower particles fall into the array, the efficiency value would not differentiate much from above η obtained with the simplest case. The performance parameter in this case is then defined as $\sqrt{\eta}$, as the sensitivity is usually inversely proportional to the square root of the number of hits, especially for showers with scarcely distributed hits at the low energies. Just because of this reason, this approach is principally for low energy gamma ray sources.

2) Array approach

As a more complex scenario, the configuration of an array of 150 m×150 m is adopted, but simulated with simplified primary particle sources - gammas and protons with fixed energies, vertically incident and bombarding at the center of the array. Analyses on angular resolution and proton-gamma discrimination are performed, so that somehow realistic performance results for each configuration are obtained. In the circumstance we are interested in, usually gamma showers generate 2–3 times more particles at the ground than that of proton with the same energy, so in the proton-gamma discrimination, the proton energy is deliberately chosen to double the energy of its gamma partner, for instance 0.5 TeV gamma versus 1 TeV proton and 1 TeV gamma versus 2 TeV proton, and so on, see Fig. 4 for the details.

In this study, an air shower cascade is simulated with Corsika v6.990 [6] and the QGSJETII model [7] is used for high energy hadronic interactions. For avoiding losing the shower information, the kinetic energy cut for secondary particles in Corsika is set to much lower values than those of the Cherenkov production threshold in the water, i.e., 50 MeV for hadrons and muons, 0.3 MeV for pions, photons and electrons. The detector is supposed to be at an altitude of 4300 m a.s.l., and the geometrical setup and the particle propagation are simulated with a code developed on the framework of Geant4 v 9.1.p01 [8].

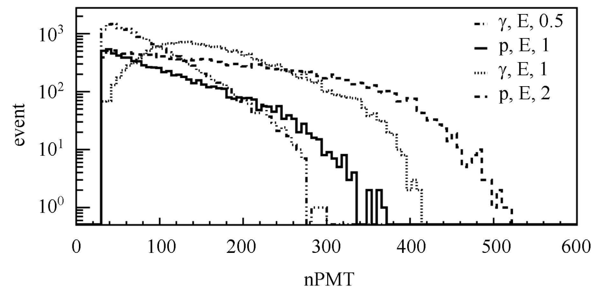

Fig. 4. Distribution of the number of hits in the case of the current official detector configuration, for primary gammas and protons at different energies, respectively.

2.2 Cost performance

The cost performance rather than the sole performance of the detector is adopted for the comparison of different configurations. Different configurations with a same array dimension may bring different costs. For example, a thicker water depth needs a higher pool bank in the construction, a larger water volume for filling up and a stronger water purification and recirculation ability in the operation, all of which requires more money; more PMTs in a cell means more PMTs to be ordered and tested, meaning more electronic channels and cables to be manufactured - that cost more money too. Assuming the detector array is fixed in the size of 150 m×150 m, the cost of every configuration is carefully evaluated, based on the engineering design reports. The performance of the detector P, here defined as the inverse of the flux sensitivity, divided by the cost C, the cost performance $P_{\rm C}$ is then calculated, that is

$$P_{\rm C}=\frac{\alpha\cdot P}{C}=\frac{\alpha\cdot Q/\theta}{C_{\rm base}+C_{\rm depth}+C_{\rm PMT}}, \quad (1)$$

where $C_{\rm base}$ is the cost of fundamental pool construction including the pond basement and the roof, which actually is a constant in this study, $C_{\rm depth}$ is the cost dependent on the water depth, $C_{\rm PMT}$ is the cost dependent on the total number of PMTs and α is a constant normalization parameter, which sets $P_{\rm C}=1$ for the case of the pool in the current official configuration, that is 5 m × 5 m in cell size, 4 m in water depth and 1 PMT in each cell. Regardless of the number of PMTs, which is taken into account already in $C_{\rm PMT}$, the cell size alone does not affect the cost much, so its contribution is trivial and ignored. Moreover, comparing with $C_{\rm base}$ and $C_{\rm PMT}$, the influence of the water depth to the cost $C_{\rm depth}$ is small. For approach 1) in the above, the performance is set to

$$P=\sqrt{\eta}, \quad (2)$$

where η is the efficiency above-mentioned. For approach 2), the performance is set to

$$P=Q/\theta, \tag{3}$$

where Q is the quality factor for proton-gamma discrimination and θ is the angular resolution to primary gammas. Those two factors are both dependent on the PMT threshold applied in the off line analysis, the P here is the maximum value while ranging the PMT threshold.

3 Simulation results

3.1 Single cell approach

A detector cell is constructed in the framework of GEANT4. 8-inch PMTs of type Hamamatsu R5912 are used, whose geometrical description and boundary effect code is taken from the GenericLAND package [9]. The water absorption length to the lights, whose dependence on wavelengths is parameterized according to the curve shape of the measurement of pure water, is scaled to 27 m at 400 nm.

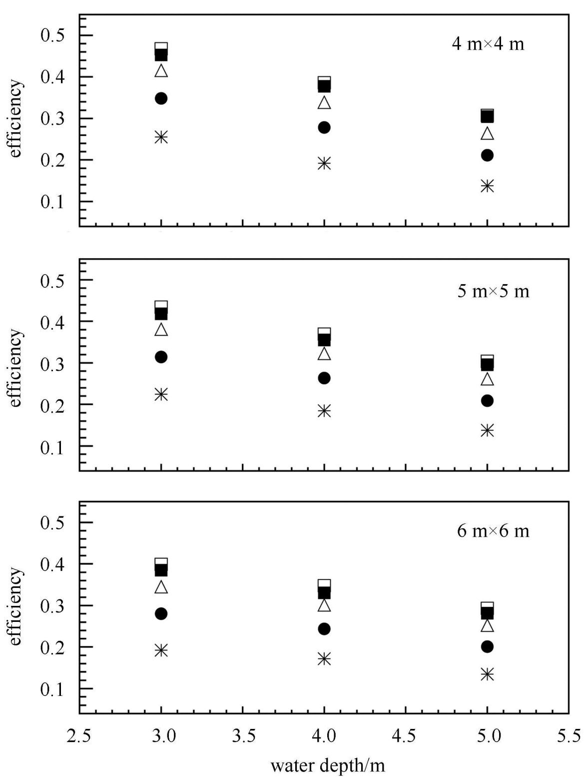

Fig. 5. Efficiency of single cell in 45 configurations. Plots in top, middle and bottom are cases for cell sizes of 4 m × 4 m, 5 m×5 m and 6 m×6 m, respectively. The abscissa is the water depth and different markers denote different groups of PMT quantities: ⋇: 1 PMT, •: 2 PMTs, △: 3 PMTs, □: 4 PMTs centered, ■: 4 PMTs scattered. The labels and markers are the same for the rest of the figures in this paper, unless otherwise explicitly mentioned.

Around 10000 showers of primary gamma at energy 1 TeV are generated in Corsika. The total number of their secondary particles arriving at the ground amounts to 10^6, most of which are photons. As to different primary energies, the energy distributions of secondary particles are eventually very close, though actually the energy of primary particles is not important at all in this study. The secondary particles are thrown and tracked in the cell detector one by one, with the particle that fires at least 1 PMT being counted; finally, the efficiency for each configuration is obtained, as shown in Fig. 5. From the plot it is seen that the efficiency is dropping while increasing the cell size, raising the water depth, or reducing the number of PMTs. For the first two trends, it can be explained as the opening angle of PMTs to tracks turning smaller, so that the chance of Cherenkov lights produced along the track hitting the PMT becomes less. The energies of air shower secondary particles are rather low, so usually the tracks of their own or of the small showers they initiate appear only at the top part of the water and have scrambled directions. The configuration with a water depth lower than 3 m is not simulated, but other studies show that there is a turning point in the efficiency curve around 3 m.

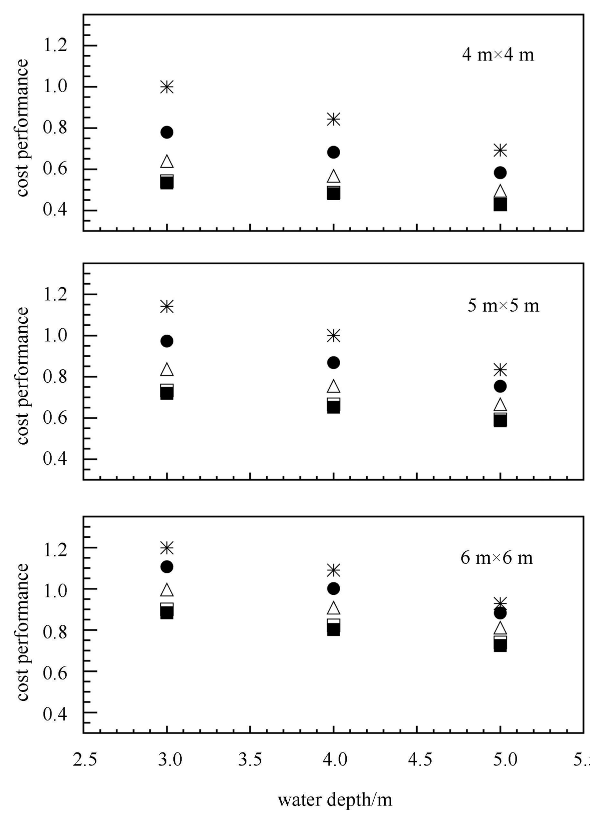

Fig. 6. Cost performance of the array in 45 configurations with the single cell approach.

The cost of the 150 m×150 m array composed of single cells in each of 45 configurations is estimated in the way mentioned in the previous section. With Eq. (1) and (2), the cost performance for each configuration is then obtained, as shown in Fig. 6. It is obvious that the group with a single PMT in a cell has a better cost performance than those of other groups. As to the water depth, due to the cost changing in the same way as the efficiency, the detector at the lower water depth has a better cost performance. It means a shallow water depth is desired for detecting low energy gamma rays. The cell size gains some 20% too when the cell size is 6 m×6 m, because of the reduction of PMT cost.

3.2 Array approach

In this approach, primary gammas with three energies, 0.5, 1 and 2 TeV, are simulated, and primary protons as the background are set to 1, 2 and 4 TeV correspondingly. For brevity, only the case of 1 TeV gamma and 2 TeV proton is introduced here. As mentioned above, the showers are vertically incident, with the core projected to the center of the array. Around 20000 gamma showers and more proton showers are simulated.

To further lessen the $P_{\rm C}$ express, the configuration with 4 PMTs scattered is abandoned. Both simulations on E/M particles and muons show no obvious differences.

3.2.1 Gamma proton discrimination

The water Cherenkov array has an extraordinary property in Gamma proton discrimination. Muons or sub-cores in hadronic showers can produce an unevenly lateral distribution of hit intensity on PMTs. When the brightest PMT outside a certain range (e.g., 45 m in radius) of the reconstructed core is chosen, using whose inverse signal amplitude ($1/cxPE$) to weight the number of fired PMTs ($nPMT$), the resulting distribution of compactness ($=nPMT/cxPE$) between gamma and proton turns quite different, especially at high energies. Tuning the threshold of compactness, the best quality factor ($Q_{\rm max}$), defined as

$$Q_{\rm max}=\frac{\xi_{\rm s}}{\sqrt{\xi_{\rm b}}}, \quad (4)$$

is found, where $\xi_{\rm s}$ and $\xi_{\rm b}$ are retained fractions of gamma and proton respectively. Fig. 7 shows the $Q_{\rm max}$ for these 36 configurations. The prominent phenomenon is that $Q_{\rm max}$ turns bigger when the water depth is higher. The reason behind this is as follows: when water depths raises, the $cxPE$ of the proton formed most by muon signals suffers little from the water depth hence keeps constant, but $nPMT$ becomes smaller due to the dropping of efficiency, as shown in the previous single cell approach; a gamma shower has very few penetrating muon particles, whose $cxPE$ are produced mainly by soft component changes, in a way very similar to $nPMT$, so the

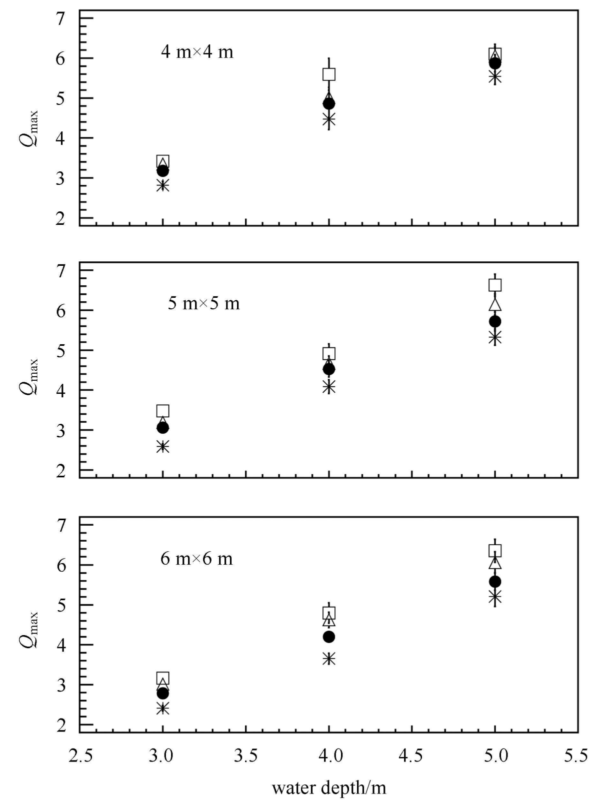

Fig. 7. The $Q_{\rm max}$ for 36 configurations of the array.

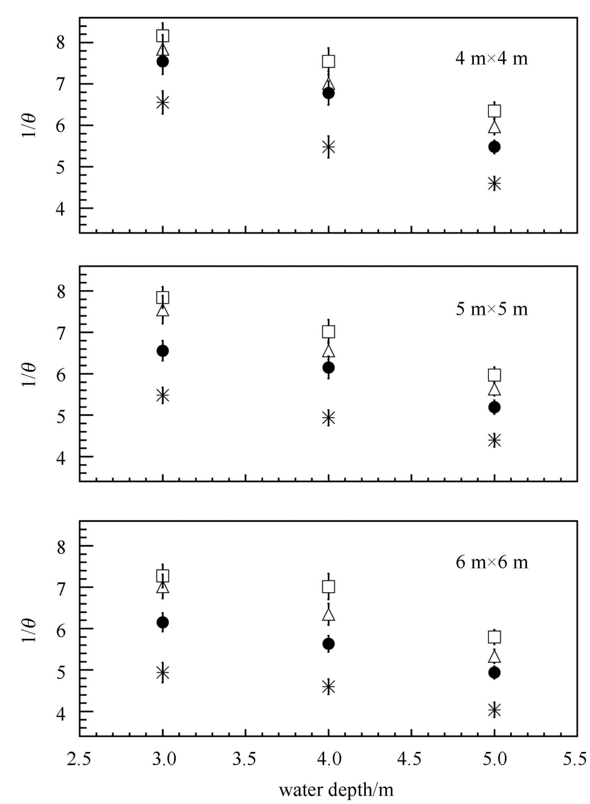

Fig. 8. Inverse angular resolution $1/\theta$ for 36 configurations of the array.

ratio $nPMT/cxPE$ varies very little.

3.2.2 Angular resolution

Only gamma showers are meaningful for this analysis. With the hit information, using the official program developed for water Cherenkov arrays, the shower direction is reconstructed. Selecting events with the compactness threshold used by the Q optimization, from the distribution of the opening angle between the reconstructed and the real directions, the angular resolution is obtained. The Rayleigh distribution is assumed so that the Gaussian-like standard deviation [10] is assigned. The plots in Fig. 8 show values $1/\theta$ for different configurations. A similar trend to the efficiency plots (Fig. 5) is observed, because the angular resolution is heavily dependent on the number of hits, which is actually determined by the efficiency.

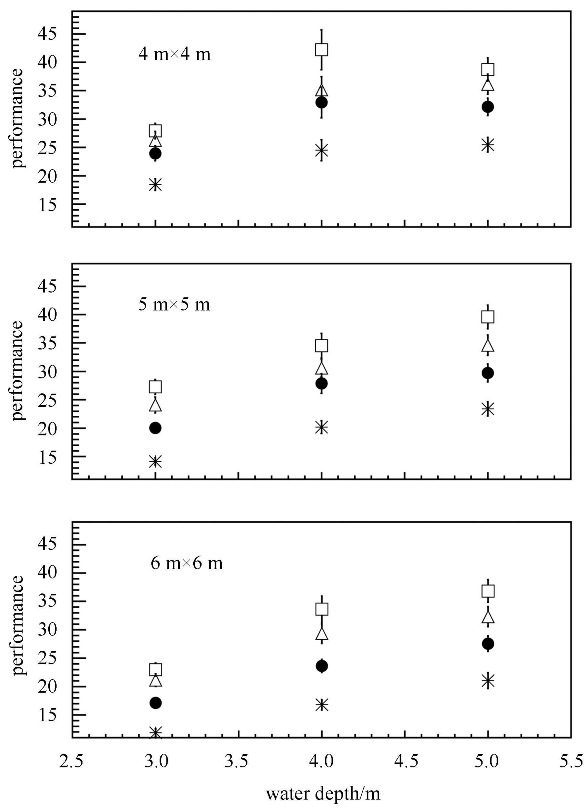

Fig. 9. Performance for 36 configurations of the array for the energy of 1 TeV gamma and 2 TeV proton.

3.2.3 Cost performance

Due to very weak dependence of the angular resolution on the compactness threshold around the optimized value, we have not bothered to optimize the performance with two factors in Eq. (3) in company. Tests to two cases of 36 configurations also show no difference at all. The performance and cost performance is finally calculated for the 36 configurations with Eq. (1) and (3), whose results are shown in Figs. 9 and 10. Controlled by the $Q_{\max}$, both the performance and cost performance turn better at a deeper water depth, totally contrasting to the trend in approach 1). If taking the statistical errors into account, configurations with less PMTs in a cell, e.g., one or two, have better cost performance. The cell size affects the cost performance too, but the influence for cases with one or two PMTs in a cell is marginal.

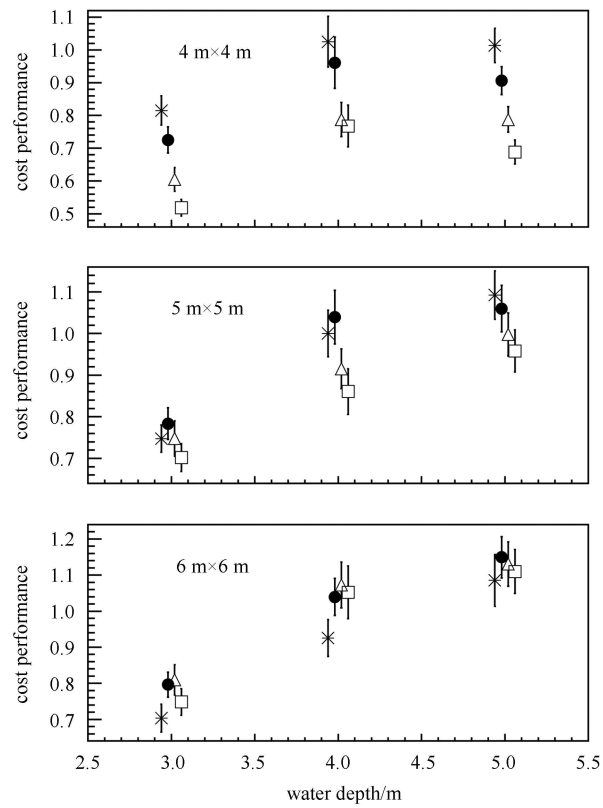

Fig. 10. Cost performance for 36 configurations of the array for the energy of 1 TeV gamma and 2 TeV proton.

4 Discussions and conclusion

Besides these simple scenarios that have been investigated, there are still some other realistic situations not being considered yet. For example, for the water quality, the absorption length 27 m at 400 nm might be too good to be maintained. If an absorption length 15 m is used, the middle plot in Fig. 10 would look like the one in Fig. 11 - the rising trend going with the water depth is depressed. Another issue is the accidentally coincident muon, which is not taken into account in the simulation. For configurations with several PMTs in a cell, the muon may fire all these PMTs altogether, troubling the reconstruction and even the trigger.

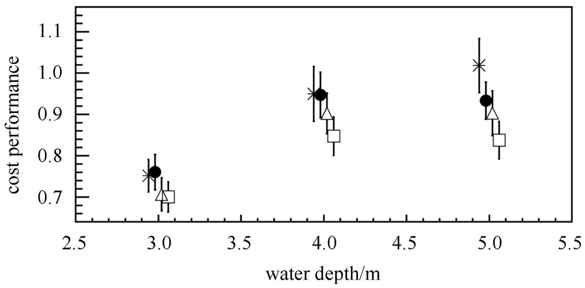

Fig. 11. Cost performance for configurations with cell size 5 m×5 m, in case the water absorption length is 15 m at 400 nm.

A bigger cell size is preferred by the simulation, no matter which approach, 1) or 2). But the difference between 5 m×5 m and 6 m×6 m is trivial, with an effect of <10%. In practice, a cell size in between can be chosen out of engineering considerations.

Contrasting results on water depth optimization are found between the two approaches. As mentioned in Section 2, these two approaches actually focus on gamma rays at different energy ranges. At low energies, gamma proton discrimination with compactness analysis does not work very well, so the angular resolution, i.e., efficiency, dominates in the performance. This point is proved by the simulation of lower primary energies in approach 2), where gamma is 0.5 TeV and proton is 1 TeV; the result shows that the 4 m rather than 5 m water depth is the best. Considering that this kind of water Cherenkov detector array is not very sensitive at low energies, such as below 1 TeV [4], it is more proper to optimize the cost performance towards higher energies - in other words, a deeper water depth is more preferred. But at the same time, the water quality issue should not be ignored. A water depth in between 4 m and 5 m should be appropriate.

No critical difference on PMT quantity selection is found in the two approaches. One PMT in a cell should be the best option.

In summary, based on this simulation work, a configuration of cell size in between 5 m×5 m and 6 m×6 m, water depth in between 4 m and 5 m, and one PMT in a cell is the best in cost performance for the water Cherenkov detector array of LHAASO.

The authors would like to express their gratitude to the Milagro Collaboration for beneficial discussions of their experiences.

References

1 Weeks T C et al. ApJ, 1989, **342**: 379–395
2 Hinton J. New J. Phys., 2009, **11**: 055005
3 Sinnis G. New J. Phys., 2009, **11**: 055007
4 YAO Z G et al. (the LHAASO collaboration). Proceedings of 32th ICRC, 2011
5 CAO Z. Chinese Physics C (HEP & NP), 2010, **34**(2): 249–252
6 http://www-ik.fzk.de/˜corsika
7 Ostapchenko S S. Nucl. Phys. B (Proc. Suppl.), 2006, **151**: 143–147; Phys. Rev. D, 2006, **74**: 014026
8 Agostinelli S et al. Nucl. Instrum. Methods in Phys. Res. A, 2003, **506**: 250–303; http://geant.cern.ch/
9 http://neutrino.phys.ksu.edu/˜GLG4sim
10 Beringer J et al. (Particle Data Group). Phys. Rev. D, 2012, **86**: 010001